Corrosion resistance of electroless Ni–low B coatings

I. Baskaran[1], T. S. N. Sankara Narayanan*[2] and A. Stephen[3]

The corrosion resistance of electroless (EL) Ni–low B coatings, obtained using an alkaline borohydride-reduced electroless plating bath, with varying concentrations of $NaBH_4$ (0·2–1·0 g L^{-1}), in 3·5%NaCl, was evaluated. The rate of deposition, boron content and the size of the nodules of the EL Ni–low B coatings were increased while the crystallinity of the coating was decreased with increasing concentration of $NaBH_4$. The change in chemical composition and decrease in crystallinity did not seem to have any influence on the corrosion resistance of the EL Ni–low B coatings of the present study, as opposed to the nodular growth with a columnar structure which had a profound effect. The results of polarisation and electrochemical impedance spectroscopy (EIS) studies confirm penetration of the corrosive medium through the columnar nature of the coating and ascertain its dominating influence on the corrosion resistance of EL Ni–low B coatings over other factors. The results of the present study again confirm the poor corrosion protective ability of EL Ni–B coatings and justify the selection of EL Ni–P coatings for applications that warrant high corrosion resistance.

Keywords: Electroless plating, Ni–low B coating, Corrosion resistance

Introduction

Electroless (EL) deposition processes have undergone numerous modifications to meet the challenging needs of a variety of industrial applications since Brenner and Riddell invented the process in 1946. Electroless Ni–high B coatings (about 5–6 wt-%B) prepared using borohydride-reduced electroless nickel plating bath offer high hardness and superior wear resistance.[1–5] The columnar structure of such coatings is useful in retaining lubricants under conditions of adhesive wear.[2] Electroless Ni–low B coatings have received considerable attention in the electronics industries due to their good solderability and their ability to act as a capping layer to prevent the diffusion of copper.[6–9] Since plating of the components used in electronics applications requires a plating bath that operates at a relatively lower temperature, DMAB-reduced electroless plating baths are commonly used for these applications. Borohydride-reduced electroless plating baths have high reduction efficiency and they are cost-effective compared to that of amine borane-based baths.[1,2] The formulation and development of an alkaline borohydride-reduced electroless nickel plating bath that operates at 45 ± 1°C, deposition of EL Ni–low B coatings using this bath and evaluation of the characteristics of the resultant coatings are addressed in the authors' earlier paper.[10] The corrosion resistance of the EL Ni–low B coatings is addressed in this paper.

Experimental

An alkaline bath having nickel chloride (30 g L^{-1}) as the source of nickel, ethylenediamine (98%) (90 g L^{-1}) and disodium tartarate (40 g L^{-1}) as complexing agents, sodium hydroxide (40 g L^{-1}) to provide the alkaline condition, sodium borohydride (0·2–1·0 g L^{-1}) as the reducing agent and thallium acetate (16 mg L^{-1}) as the stabiliser, was used to prepare the EL Ni–low B coatings. The pH and temperature of the plating bath were maintained at 13 and 45 ± 1°C respectively. The details regarding the determination of plating rate, chemical composition, morphological features and structural characteristics have already been described previously by the authors.[10] The plating rate of EL Ni–low B coating was determined gravimetrically based on the gain in weight after depositing the coating on copper substrates (electrolytic grade, $40 \times 20 \times 2$ mm). Before plating, the copper substrates were degreased with acetone, cleaned using 1 : 1 HNO_3, washed thoroughly with deionised water and activated using Watt's nickel bath. The boron content of the EL Ni–low B coatings was determined by inductively coupled plasma-optical emission spectrometry (PerkinElmer Optima 5300DV), whereas the nickel content was determined by gravimetric method after precipitating the nickel as Ni–DMG complex. The surface morphology of EL Ni–low B coatings was assessed using scanning electron

[1]Department of Materials Engineering, Technical University of Lisbon, Instituto Superior Tecnico, Av. Rovisco Pais, 1049-001 Lisbon, Portugal
[2]National Metallurgical Laboratory, Madras Centre, CSIR Complex, Taramani, Chennai 600 113, India
[3]Materials Science Centre, Department of Nuclear Physics, University of Madras, Chennai 600 025, India

*Corresponding author, email tsnsn@rediffmail.com

Published by Maney on behalf of the Institute
Received 11 November 2008; accepted 15 March 2009
DOI 10.1179/174591909X438848

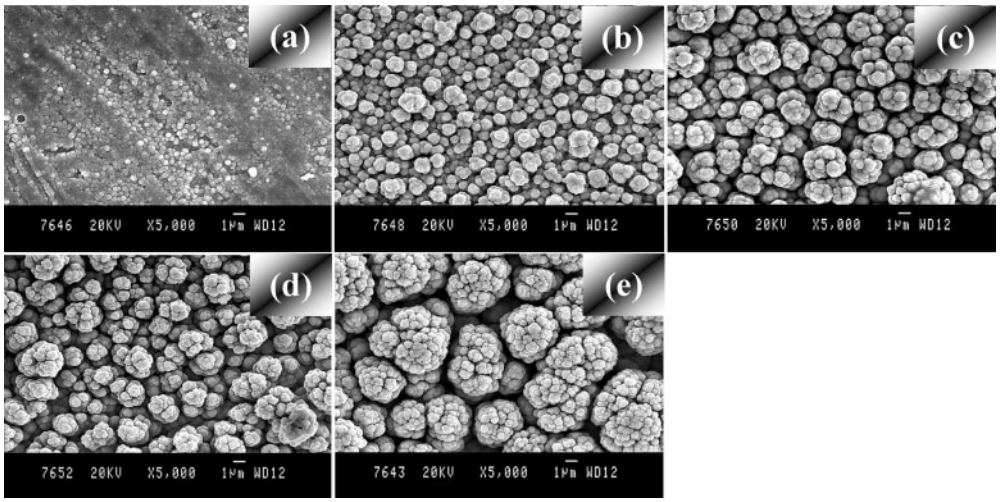

a NB2; *b* NB4; *c* NB6; *d* NB8; *e* NB10

1 Surface morphology of EL Ni–low B coatings obtained using 0·2, 0·4, 0·6, 0·8 and 1 g L^{-1} $NaBH_4$

microscope [Cambridge scanning electron microscope (S360) with EDAX attachment]. The structural characteristics of EL Ni–low B coatings was determined using X-ray diffraction (XRD) measurements (Rich Seifert, Germany; Model 3000), using Cu K_α radiation. The corrosion resistance of EL Ni–low B coatings, deposited on mild steel substrates, in 3·5 wt-%NaCl, was evaluated by potentiodynamic polarisation and electrochemical impedance spectroscopy (EIS) studies using a potentiostat/galvanostat/frequency response analyser (ACM Instruments, UK; Model Gill AC). The thickness of the EL Ni–low B coatings used for evaluating the corrosion resistance was 15 ± 3 μm. The EL Ni–low B coated mild steel was used as the working electrode while a saturated calomel electrode and a graphite rod served as the reference and counter electrodes respectively. These electrodes were placed inside a flat cell in such a way that only 1 cm^2 area of the working electrode was exposed to the electrolyte solution and the tip of the Luggin probe is closer ($\sim$2 mm) to the working electrode. Potentiodynamic polarisation studies were performed at a scan rate of 100 mV min^{-1}. The corrosion potential E_{corr} and corrosion current density i_{corr} were determined from the polarisation curves using the Tafel extrapolation method. Electrochemical impedance spectroscopy (EIS) studies of EL Ni–low B coatings were performed at their respective open circuit potentials. The charge transfer resistance R_{ct} and double layer capacitance C_{dl} were determined from the Nyquist plots by fitting the data using Boukamp software. The Bode plots were also analysed to understand the mechanism of corrosion of EL Ni–low B coated mild steel in 3·5%NaCl.

Results and discussion

Characteristics of EL Ni–low B coatings

The EL Ni–low B coatings obtained using 0·2, 0·4, 0·6, 0·8 and 1·0 g L^{-1} $NaBH_4$ are designated as NB2, NB4, NB6, NB8 and NB10 respectively. The plating rate, chemical composition, structural and morphological characteristics of these coatings have already been described in an earlier paper.[10] The rate of deposition and boron content of EL Ni–low B coatings are increased, from 1·40 to 10·20 μm h^{-1} and from 0·6 to 3·2 wt-% respectively, with increasing $NaBH_4$ concentration from 0·2 to 1·0 g L^{-1}. The rate of deposition from these baths is relatively lower compared with those obtained using a borohydride-reduced electroless plating baths operated at 95 ± 1°C.[4,5] Hence, for preparing EL Ni–low B coatings with a thickness of 15 ± 3 μm, it requires about 780, 240, 180, 120 and 100 min. (with continuous replenishment) using a $NaBH_4$ concentration of 0·2, 0·4, 0·6, 0·8 and 1·0 g L^{-1} respectively. The surface morphology of EL Ni–low B coatings resembles a typical cauliflower type feature.[4–6,10–12] The size of the nodules increased with increasing $NaBH_4$ concentration from 0·2 to 1·0 g L^{-1} (Fig. 1). The structural characteristics of EL Ni–low B coatings, evaluated by XRD measurements, suggest that the crystallinity of the coating is decreased with increasing $NaBH_4$ concentration from 0·2 to 1·0 g L^{-1}.[10]

Corrosion behaviour of EL Ni–low B coatings

The potentiodynamic polarisation curves of EL Ni–low B coated mild steel in 3·5%NaCl are shown in Fig. 2. The corrosion potential E_{corr} and corrosion current density i_{corr}, calculated using the Tafel extrapolation method, are compiled in Table 1. There is observed to be a slight cathodic shift in E_{corr} when the boron content of the EL Ni–low B coating is increased from 0·6 to 1·2 wt-% (from NB2 to NB4). However, the i_{corr} of these two coatings lie closer to each other. Increase in boron

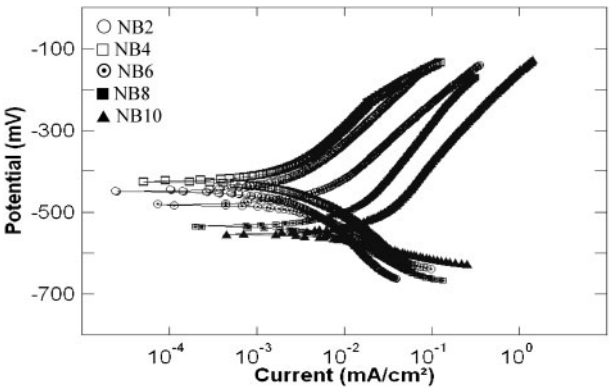

2 Potentiodynamic polarisation curves of EL Ni–low B coatings in 3·5%NaCl: potentials in mV(SCE)

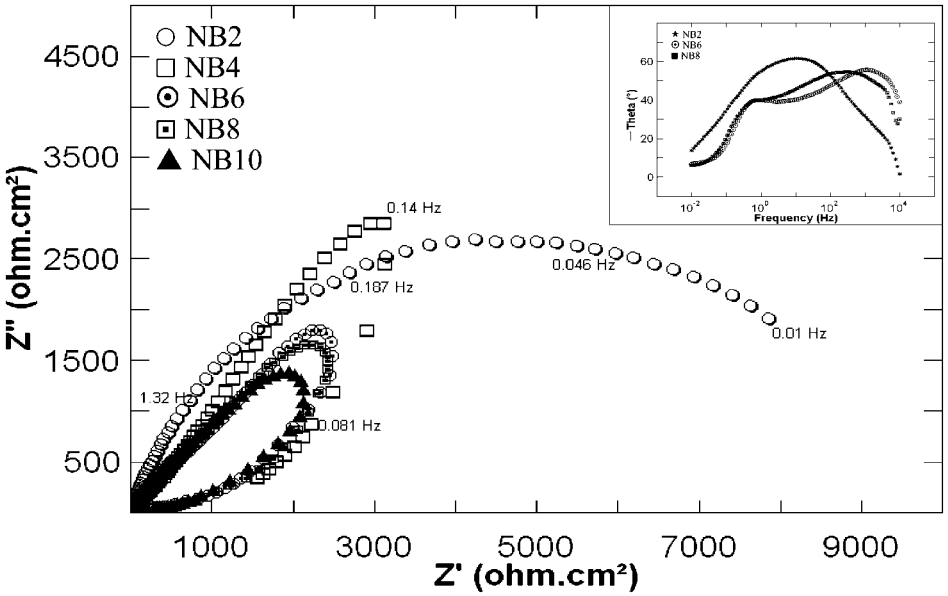

3 Nyquist and Bode (inset) plots of EL Ni–low B coatings in 3·5%NaCl at their respective open circuit potentials

content of the EL Ni–low B coatings beyond 1·2 wt-% exhibits a reversal in trend. The E_{corr} shifts towards more negative values, from −424 to −554 mV(SCE) when the boron content of the EL Ni–low B coating is increased from 1·2 to 3·2 wt-% (from NB4 to NB10) with a corresponding increase in the i_{corr} from 1·7 to 6·8 μA cm^{-2}. The predominant reactions that could occur during the cathodic and anodic polarisation of coated mild steel are the reduction of oxygen and iron dissolution respectively. The rate at which these two reactions occur determines the corrosion resistance. The shift in E_{corr} towards more negative values with a corresponding increase in i_{corr} observed for electroless Ni–low B coated mild steel suggests the increase in electrochemical activity for cathodic and anodic reactions. The change in shape of the polarisation curves further supports this view.

The Nyquist plots of EL Ni–low B coated mild steel in 3·5%NaCl, at their respective open circuit potentials, is shown in Fig. 3. The R_{ct} and C_{dl} values, calculated after fitting the data using Boukamp software, are given in Table 1. In general, a high value of R_{ct} implies a better corrosion protective ability of the coating. In the present study, the R_{ct} value of the EL Ni–low B coating is increased from 8868 to 9520 Ω cm^2 when the boron content of the coating is increased from 0·6 to 1·2 wt-% (from NB2 to NB4). However, further increase in boron content of the coating beyond 1·2 wt-% exhibits a reversal in trend. The R_{ct} value is decreased from 9520 to 7034 Ω cm^2 when the boron content of the EL Ni–low B coating is increased from 1·2 to 3·2 wt-% (from NB4 to NB10). The C_{dl} value is related to the porosity of the coating.[13] The C_{dl} value of the EL Ni–low B coating is decreased from 150 to 133 μF when the boron content of the coating is increased from 0·6 to 1·2 wt-% (from NB2 to NB4). However, further increase in boron content of the coating beyond 1·2 wt-% exhibits a reversal in trend. The C_{dl} value is increased from 133 to 196 μF when the boron content of the EL Ni–low B coating is increased from 1·2 to 3·2 wt-% (from NB4 to NB10). The corrosion performance of EL Ni–low B coatings observed by EIS studies strongly supports observations made by potentiodynamic polarisation studies.

Several factors, which include thickness, porosity, composition of the coating, structure, heterogeneity of the coating and nodular features with a columnar growth of the coating, could influence the corrosion resistance of electroless plated coatings. Since the thickness of the EL Ni–low B coatings used in the present study is 15 ± 3 μm, the contribution from the coating porosity is expected to be minimal. The EL Ni–low B coatings exhibit variation in their composition (Table 1), which also reflects in their structure. The EL Ni–low B coating NB2 is fully crystalline whereas NB10 is microcrystalline in nature.[10] As the codeposition of thallium in all the EL Ni–low B coatings studied is about 0·1–0·2 wt-%, the surface heterogeneity induced by the codeposition of thallium is likely to be similar in all the cases studied. Surface morphological features

Table 1 Corrosion resistance of EL Ni–low B coatings* in 3·5%NaCl solution, evaluated by potentiodynamic polarisation and electrochemical impedance spectroscopy (EIS) studies

Designation of the EL Ni–low B coating	Nickel content, wt-%	Boron content, wt-%	E_{corr}, mV(SCE)	i_{corr}, μA cm^{-2}	R_{ct}, Ω cm^2	C_{dl}, μF
NB2	99·3	0·6	−449	1·8	8868	150
NB4	98·7	1·2	−424	1·7	9520	133
NB6	97·9	2·0	−482	2·7	8470	159
NB8	97·2	2·6	−534	5·2	7440	187
NB10	96·6	3·2	−554	6·8	7034	196

*Thallium contents of all these coatings are in the range of 0·1–0·2 wt-%.

indicate that with the exception of NB2, the remaining coatings exhibit a nodular growth with a columnar structure; the nodule size increases with increasing boron content of the coating.[10]

The Nyquist plots of the EL Ni–low B coating, NB2, exhibits only a single semicircle whereas the other four coatings (from NB4 to NB10) exhibit a semicircle in the high frequency region followed by a loop in the low frequency region. For EL Ni–low B coatings from NB4 to NB10, the curves in the Nyquist plot appear to be similar with respect to their shape, but they differ considerably in their size. This indicates that the same fundamental process must be occurring on all these coatings but over a different effective area in each case. The formation of a single semicircle or a semicircle in the high frequency region followed by a low frequency loop is typical of metallic coatings. The semicircle at high frequency region represents the coating response, while the loop at low frequency region is associated with simultaneous physicochemical phenomena that occur at the metal/coating/solution interface.[12,14–17] According to Mansfeld *et al.*,[17] the loop at low frequency region is associated with the double layer capacitance and/or diffusion phenomena of the oxidant chemical species through a porous coating.

In order to get a better insight about the coating response as well as the diffusion phenomenon, Bode plots ($\log f$ *v.* $\log |Z|$ and $\log f$ *v.* phase angle) are constructed. The EL Ni–low B coating NB2 exhibits a single phase angle maximum in the plot of $\log f$ *v.* phase angle (inset of Fig. 3), suggesting that the corrosion process involves only a single time constant. However, in the case of the other four EL Ni–low B coatings (from NB4 to NB10), the Bode plots indicate the presence of two phase angle maximum (inset of Fig. 3), suggesting the involvement of two time constants. The two phase angle maximums could be related to the electrolyte/coating and the electrolyte/substrate interfaces. The occurrence of the second phase angle maximum for the EL Ni–low B coatings NB4, NB6, NB8 and NB10 clearly indicates that the electrolyte has penetrated via the granular structure in these coatings to create another interface, namely, electrolyte/substrate interface. The nodular growth with a columnar structure of the EL Ni–low B coatings from NB4 to NB10 enables the electrolyte to penetrate through them. The Bode plots (inset of Fig. 3) also indicate the involvement of a diffusion phenomenon for all the coatings in the low frequency regions.

The effect of increase in boron content and decrease in crystallinity of the coating which are expected to offer an improvement in corrosion resistance in EL Ni–high B coatings is not realised in the EL Ni–low B coatings of the present study. The influence of increase in boron content and decrease in crystallinity of the coating on the corrosion resistance of EL Ni–B coatings is nullified by the morphological features of the EL Ni–low B coatings, nodular growth with a columnar structure, which allows transport of the corrosive medium through them. The reversal in E_{corr} and i_{corr} values, the occurrence of semicircle in the high frequency region followed by a loop in the low frequency region in the Nyquist plot and the occurrence of the second phase angle maximum in the Bode plot, for EL Ni–low B coatings obtained using $>0{\cdot}4$ g L^{-1} $NaBH_4$, confirm penetration of the corrosive medium through the columnar nature of the coating and establish its dominating influence on the corrosion resistance of EL Ni–low B coatings over other factors.

Conclusion

The rate of deposition of EL Ni–low B coatings is increased from 1·40 to 10·20 μm h^{-1} when the concentration of $NaBH_4$ in the plating bath is increased from 0·2 to 1·0 g L^{-1}, with a corresponding increase in the boron content of the coating from 0·6 to 3·2 wt-%. The morphology of the EL Ni–low B coatings exhibits a nodular feature that resembles a typical cauliflower type structure in which the size of the nodules increases with increasing concentration of $NaBH_4$. The influence of increase in boron content and decrease in crystallinity is not reflected in the corrosion resistance of the EL Ni–low B coatings. The influence of these factors is nullified by the morphological features of the EL Ni–low B coatings, nodular growth with a columnar structure, which allows transport of the corrosive medium through them. The reversal in E_{corr} and i_{corr} values, the occurrence of semicircle in the high frequency region followed by a loop in the low frequency region in the Nyquist plot and the occurrence of the second phase angle maximum in the Bode plot, for EL Ni–low B coatings obtained using $>0{\cdot}4$ g L^{-1} $NaBH_4$, confirm penetration of the corrosive medium through the columnar nature of the coating and ascertain its dominating influence on the corrosion resistance of EL Ni–low B coatings over other factors. The results of the present study confirm again the poor corrosion protective ability of EL Ni–B coatings and justify the selection of EL Ni–P coatings for applications that require high corrosion resistance.

References

1. K. M. Gorbunova, M. V. Ivanov and V. P. Moissev: *J. Electrochem. Soc.*, 1973, **120**, 613.
2. R. N. Duncan and T. L. Arney: *Plat. Surf. Finish.*, 1984, **71**, 49.
3. T. S. N. Sankara Narayanan, K. Krishnaveni and S. K. Seshadri: *Mater. Chem. Phys.*, 2003, **82**, 771.
4. T. S. N. Sankara Narayanan and S. K. Seshadri: *J. Alloys Compd*, 2004, **365**, 197.
5. K. Krishnaveni, T. S. N. Sankara Narayanan and S. K. Seshadri: *Surf. Coat. Technol.*, 2005, **190**, 115.
6. S. M. Ho, S. M. Lian, K. M. Chen, J. P. Pan, T. H. Wang and A. Hung: *IEEE Trans. Compon. Packaging Manuf. Technol. A*, 1996, **19A**, (2), 202.
7. Y. M. Chow, W. M. Lau and Z. S. Karim: *Surf. Interf. Anal.*, 2001, **31**, 321.
8. M. Tsukimura, H. Inoue, H. Ezawa, M. Miyata and M. Ota: *Mater. Trans.*, 2002, **43**, (7), 1615.
9. T. Osaka, N. Takano, T. Kurokawa, T. Kaneko and K. Ueno: *Surf. Coat. Technol.*, 2003, **169–170**, 124.
10. I. Baskaran, R. Sakthi Kumar, T. S. N. Sankara Narayanan and A. Stephen: *Surf. Coat. Technol.*, 2006, **200**, 6888.
11. F. Delaunois, J. P. Petitjean, P. Lienard and M. Jacob-Duliere: *Surf. Coat. Technol.*, 2000, **124**, 201.
12. F. Delaunois and P. Lienard: *Surf. Coat. Technol.*, 2002, **160**, 239.
13. J. Flis and D. J. Duquette: *Corrosion*, 1985, **41**, 700.
14. A. Atkinson and D. W. Smart: *J. Electrochem. Soc.*, 1988, **135**, 2886.
15. J. N. Balaraju, T. S. N. Sankara Narayanan and S. K. Seshadri: *J. Solid State Electrochem.*, 2001, **5**, 334.
16. P. H. Lo, W. T. Tsai, J. T. Lee and M. P. Hung: *J. Electrochem. Soc.*, 1995, **142**, 91.
17. F. Mansfeld, M. Kending and S. Tsai: *Corrosion*, 1982, **38**, 478.